AIP | Journal of Applied Physics

Interfacial thermal resistance between metallic carbon nanotube and Cu substrate

Feng Gao, Jianmin Qu, and Matthew Yao

Citation: J. Appl. Phys. **110**, 124314 (2011); doi: 10.1063/1.3670011
View online: http://dx.doi.org/10.1063/1.3670011
View Table of Contents: http://jap.aip.org/resource/1/JAPIAU/v110/i12
Published by the American Institute of Physics.

Interfacial thermal resistance between metallic carbon nanotube and Cu substrate

Feng Gao,[1] Jianmin Qu,[1,2,a)] and Matthew Yao[3]
[1]*Department of Civil and Environmental Engineering, Northwestern University, Evanston, Illinois 60208, USA*
[2]*Department of Mechanical Engineering, Northwestern University, Evanston, Illinois 60208, USA*
[3]*Rockwell Collins Inc., Cedar Rapids, Iowa 52498, USA*

(Received 7 September 2011; accepted 12 November 2011; published online 21 December 2011)

A comprehensive model was developed to calculate the interfacial thermal resistance between a metallic carbon nanotube (CNT) and a Cu substrate. The new model accounts for both phonon-mediated and electron-mediated thermal transfer at the interface, as well as the effect of electron-phonon coupling within CNT and Cu. The phonon-mediated thermal transfer was simulated using the non-equilibrium molecular dynamics, while the electron-mediated thermal transfer was computed by the non-equilibrium Green's function method in conjunction with the density function theory. The effect of electron-phonon coupling within Cu and CNT was investigated by using the kinetic theory. Our results show that (1) electron-phonon coupling within Cu and CNT contributes significantly to the overall thermal transfer across the CNT/Cu interface, and (2) contributions to the overall thermal conductance at the CNT/Cu interface from the electron-mediated thermal transfer are comparable to that from the phonon-mediated thermal transfer. © *2011 American Institute of Physics*. [doi:10.1063/1.3670011]

I. INTRODUCTION

Thermal resistance across material interfaces is a critical consideration in a variety of scientific and engineering applications. As the power density in electronic devices increases, thermal management becomes more challenging. For example, in many high power devices, thermal resistance between the chip and the heat sink may account for as much as half of the total thermal budget. Consequently, chip-level heat dissipation is a crucial bottleneck hindering the development of advanced microelectronics with high junction temperatures. Due to their high thermal conductance (up to 3000 W/mK), carbon nanotube (CNT) is a natural choice for the thermal interface material (TIM) to overcome the limitation on heat dissipation. Early attempts used CNTs as fillers to form high thermal conductivity fluids or TIM composites.[1–3] However, this approach is not effective due to the random dispersion of CNTs and the intermittent link among the CNTs. A more advanced approach is to grow CNTs vertically on a silicon wafer. These vertically aligned CNTs can be attached to a copper heat spreader to form a thermal interface structure.[4–7]

To understand the fundamental physics of heat transfer across the interfaces in the Si/CNT/Cu assembly, atomic-level simulations have been used to calculate the interfacial thermal resistance. In particular, the interfacial thermal resistance between CNT and Si (or SiO_2) substrate has been studied using molecular dynamics (MD).[8–11] It was found that the external pressure increases the contact area between CNT and Si, and thus enhances the thermal conductance at the interface.[8] The larger number of chemical bond between a vertical CNT tube and the Si substrate can improve not only the interfacial adhesion but also the interfacial thermal conductance.[9]

All the aforementioned MD simulations were carried out based on the assumption that thermal transfer across the interface is mediated predominantly by phonon-phonon coupling. This may be reasonable for the CNT/Si interface, as electron transport across the CNT/Si interface is extremely limited. At the metallic CNT/Cu interface, electron-mediated thermal transfer may also play an important role on the thermal transfer across the CNT/Cu interface. This conjecture is based on the remarkable electron transmission coefficient across the CNT/Cu interface at room temperature (e.g., 300 K).[12] In addition, it has been reported that the electron-phonon coupling within metal bulk substrate also plays a significant role on the thermal conductance at the metal/nonmetal interface.[13,14] In other words, total thermal transfer at metallic CNT/metal interfaces may be mediated by both phonons and electrons. To account for the electron-mediated thermal transfer, Li *et al.*[14] proposed an additional thermal path, namely, the direct electron-electron coupling at the metal/CNT interface, and the subsequent coupling between the electrons and phonons within the CNT tube. Although the electron-mediated thermal transfer at metal/metal interfaces has been investigated,[15] electron-mediated thermal transfer across the metallic CNT/metal interface has not been fully understood yet.

To this end, this paper is to develop a model that enables the calculating of the total thermal conductance at the metallic CNT(10,10)/Cu interface, by accounting for the following contributions: (1) electron-phonon coupling within the Cu substrate; (2) phonon-phonon coupling at the CNT/Cu interface; (3) electron-electron coupling at the CNT/Cu interface; and (4) electron-phonon coupling within the CNT tube.

a)Author to whom correspondence should be addressed. Electronic mail: j-qu@Northwestern.edu. FAX: 847-491-4011.

II. THERMAL TRANSFER PATHS ACROSS CNT/Cu INTERFACE

Both phonons and electrons can act as heat carriers to transfer heat across a CNT/Cu interface.[13,14,16] Thus, the following physical model is proposed in this study to calculate the total interfacial thermal resistance between a metallic CNT and a metal substrate.

Shown in Fig. 1 is a schematic diagram of the possible thermal transfer paths at a CNT(10,10)/Cu interface. Path-I is the phonon-mediated path, along which heat carried by electrons in the Cu is passed on to phonons within the Cu. Then, at the interface, heat is further transferred from phonons in the Cu to phonons in the CNT. As shown in Fig. 1, thermal resistance associated with these two heat transfer processes is denoted by $R_{Cu(e-p)}$ and R_{p-p}, respectively. Since these two processes are in series,[13,14,17] the total thermal resistance along Path-I is give by

$$R_I = R_{Cu(e-p)} + R_{p-p}. \tag{1}$$

We note that R_I has been studied based on the diffuse mismatch model combined with the kinetic theory, accounting for the electron-phonon coupling at the metal/non-metal interface.[13]

Path-II is the electron-mediated path along which heat carried by the electrons in the Cu is first passed on to the electrons in the CNT at the CNT/Cu interface. Once within the CNT, heat carried by the electrons in the CNT is transferred on to phonons. Thus, if R_{e-e} and $R_{CNT(e-p)}$ are used to represent the resistances associated with these two thermal transfer processes, the total thermal resistance along Path-II can be written as

$$R_{II} = R_{e-e} + R_{CNT(e-p)}. \tag{2}$$

Since Path-I and Path-II are in parallel,[16] the total resistance of the interface R_{total} can be written as

$$\frac{1}{R_{total}} = \frac{1}{R_I} + \frac{1}{R_{II}}, \tag{3}$$

Conceptually, there should be a third path representing the direct interfacial heat transfer from electrons in the Cu to the phonons in the CNT. However, experimental data have shown that direct coupling between electrons in the metal and phonons in the CNT at the CNT/Cu interface is negligible compared to the other contributions shown in Fig. 1.[18,19] Thus, this electron-phonon coupling at the CNT/Cu interface will not be included in our model.

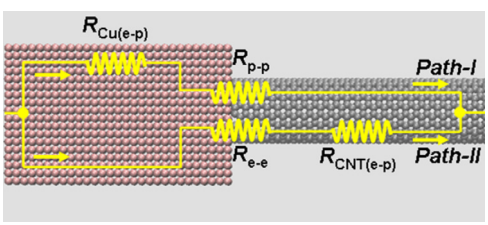

FIG. 1. (Color online) Thermal transfer paths at the interface between a metallic CNT(10,10) and Cu substrate.

III. RESULTS AND DISCUSSION

A. Thermal resistance along Path I

To calculate $R_I = R_{Cu(e-p)} + R_{p-p}$, we first focus on $R_{Cu(e-p)}$, which is the energy (heat) loss when heat carried by the electrons is passed on to phonons. The corresponding thermal conductance $\kappa_{Cu(e-p)}$ of this thermal transfer process can be described by the kinetic theory,[13] i.e.,

$$\kappa_{Cu(e-p)} = \frac{1}{R_{Cu(e-p)}} = \sqrt{G \cdot k_{p(Cu)}} = \sqrt{\left(C_{e(Cu)} \cdot \tau\right) \cdot \kappa_{p(Cu)}}, \tag{4}$$

where G is the electron cooling rate (or electron to phonon energy transfer per unit volume), $C_{e(Cu)}$ is the electron heat capacity per unit volume, τ is the relaxation time characterizing electron-phonon energy loss or electron cooling, and $\kappa_{p(Cu)}$(in W/mK) is phonon or lattice thermal conductivity of Cu. All these physical parameters are associated with Cu.

First, the electron-mediated thermal conductivity in Cu can be calculated using the Wiedemann-Franz law

$$\frac{\kappa_{e(Cu)}}{\sigma} = L \cdot T, \tag{5}$$

where $\kappa_{e(Cu)}$ is the electronic contribution to the thermal conductivity, σ is the electrical conductivity of the metal, T is the temperature, and L is the Lorenz factor. For Cu at 300 K, the total thermal conductivity is $\kappa = 401$ W/mK, while the electrical conductivity is $\sigma = 1/(1.70 \times 10^{-8})\Omega m^{-1}$.[20] The Lorenz factor L for Cu is $L = 2.23$ V^2/K^2. The electron-mediated thermal conductivity is then calculated from (5), $\kappa_{e(Cu)} = 394$ W/mK at 300 K. Thus, the phonon-mediated thermal conductivity $\kappa_{p(Cu)} = \kappa - \kappa_{e(Cu)}$ is equal to approximate 7 W/mK.

In Eq. (4), $C_{e(Cu)}$ is the electron heat capacity per unit volume, which is about 10^4 J/cm^3 K for Cu.[13] The relaxation time τ was measured by pulse laser $\tau = 1 \sim 4$ ps.[21] In this study, τ is taken as 1 ps to capture the possible maximum thermal resistance associated with this electron-phonon coupling effect. The thermal conductance $\kappa_{Cu(e-p)}$ is then calculated as 840 W/mm^2 K. This is comparable to the value caused by the phonon-phonon coupling at the CNT/Cu interface, which will be calculated later.

To calculate the thermal resistance caused by phonon-phonon scattering at the metallic CNT/Cu interface, the non-equilibrium molecular dynamics (NEMD) is employed in this study. This method has been widely used to calculate the thermal conductance for both CNT tube[22–26] and CNT/substrate junctions.[8,9,11]

Shown in Fig. 2 is the simulation cell of a CNT(10,10) tube with each end in contact with a Cu substrate. Periodic

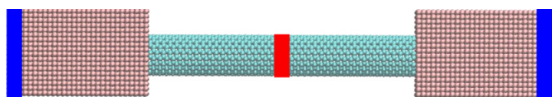

FIG. 2. (Color online) The Cu/CNT(10,10)/Cu sandwich model for NEMD simulations. The red-domain at the center of CNT tube represents the hot reservoir while the dark blue domains at the ends of Cu blocks denote the cold reservoirs.

boundary conditions are prescribed in all directions. Random initial velocities are assigned to individual atoms to approximate the target temperature of the system (e.g., 300 K). A certain amount of heat flux is applied in the middle of CNT tube to generate a heat source, while the same amount of heat flux is removed from the opposite ends of the Cu substrates. The method used here is similar to that developed by Jund and Jullien.[27] The Tersoff[28,29] and Brenner[30] interatomic potentials have been widely used to describe the C-C covalent bonds and calculate the thermal conductivity of CNT and graphene. Recently, however, it has been reported that the original Tersoff and Brenner interatomic potentials cannot predict the phonon dispersions accurately.[31] Consequently, the calculated thermal conductivity of CNT or graphene is much lower than the experimental results. In this study, the optimized Tersoff interatomic potential[31] is used to describe the phonon dispersions and thermal conductivity of CNT and graphene. The modified embedded atom method potential is used to describe the interaction among the atoms in the Cu substrate.[32] To describe the Cu-C interaction, a Morse potential is used to capture the possible chemical bond at the CNT/Cu interface.[33]

All the MD simulations were performed using the LAMMPS code to integrate the equations of motion with a velocity-verlet algorithm and a 0.5 fs time step. First, a Nose-Hoover thermostat is prescribed for 50 fs to equilibrate the system temperature and relax the structure. Second, the system is allowed to run for 250 ps in the microcanonical ensemble, where the atomic velocities are recorded and averaged over the final 75 ps. Finally, the temperatures is computed according to the equipartition theorem[26]

$$T = \frac{1}{3Nk_B}\sum_{1}^{n} m_i v_i^2, \tag{6}$$

where N is the number of atoms in the local domain, k_B is the Boltzmann's constant, m_i is the atomic mass, and v_i is the atomic velocity. Local temperature is averaged spatially and temporally in order to visualize the approximate steady-state distribution of temperature across the entire system.

A typical temperature profile across the entire system is shown in Fig. 3. It is seen that, as expected, the highest temperature occurs in the middle of the CNT tube where the heat source is originally located, and the lowest temperature is at the ends of Cu substrate where the heat flux is removed. Furthermore, the temperature gradients within the CNT tube and the Cu substrates are relatively small in comparison to the temperature drops across the CNT/Cu interfaces, indicating that thermal resistance of the system is primarily at the CNT/Cu interfaces.

To understand the mechanisms of the interfacial resistance, the total phonon density of states (DOS)[9] is investigated. The phonon DOS can be calculated directly from the Fourier transform of the velocity autocorrelation function under quasi-harmonic approximation,[34,35]

$$\frac{3Nk_BT}{V} = \int_0^{\omega_{\max}} C \cdot D(\omega) n(\omega, T) \hbar\omega d\omega, \tag{7}$$

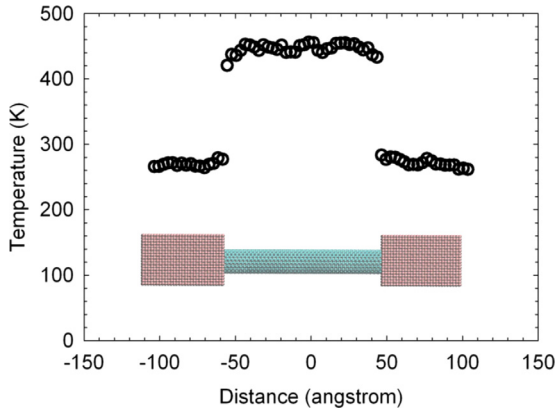

FIG. 3. (Color online) Calculated temperature profile across a Cu/CNT(10,10)/Cu sandwich system at 300 K. The inset is the corresponding Cu/CNT/Cu model used for the MD simulations.

where $\hbar$ is the Planck's constant, C is a scaling factor, N is the number of atoms, V is the volume of the system, $D(\omega)$ is the phonon DOS as a function of frequency ω, $n(\omega, T)$ is the Bose-Einstein occupation number given by[34]

$$n(\omega, T) = \frac{1}{2} + 1 \Big/ \left(e^{\frac{\hbar\omega}{k_B T}} - 1\right). \tag{8}$$

The group velocity is calculated as the weighted average of each acoustic mode velocity as it appears in the Debye density of states. For CNT(10,10) tube, there are three acoustic mode velocities, longitudinal-acoustic ($v_{LA} = 20.35$ km/s), transverse-acoustic ($v_{TA} = 9.43$ km/s), and a twist mode ($v_{TW} = 15.0$ km/s). The average of these group velocities are calculated from[34]

$$\frac{4}{v_{ave}^3} = \frac{1}{v_{LA}^3} + \frac{2}{v_{TA}^3} + \frac{1}{v_{TW}^3}. \tag{9}$$

The result is $v_{ave} = 11.26$ km/s.

In addition, the mode velocities of the Cu substrate are obtained from the study by Swartz and Pohl.[36] Figure 4 shows the comparison of the calculated phonon DOS between CNT(10,10) and Cu. The overlapped area between the phonon DOS of the CNT and that of the Cu gives a qualitative measure of the phonon-phonon coupling[9] at the CNT/Cu interface. It is seen from Fig. 4 that except in the frequency range (0–6 THz), the phonon DOS has no overlap between CNT and Cu, indicating potentially a large thermal resistance at the CNT/Cu interface.

The relation between the prescribed heat flux Q and the temperature drop ΔT is given by

$$Q = \kappa_{p-p}\Delta T, \tag{10}$$

where κ_{p-p} is the Kapitza conductance mediated by phonon transfer. The inverse of it is the interfacial thermal resistance due to phonon scattering at the interface. Since Q is a known input parameter, and ΔT can be obtained from the temperature profile, see Fig. 3, the Kaptiza conductance can then be calculated from (10), i.e., $\kappa_{p-p} = 296$ W/mm^2 K.

Finally, the total thermal resistance along Path-I can be determined by Eq. (1)

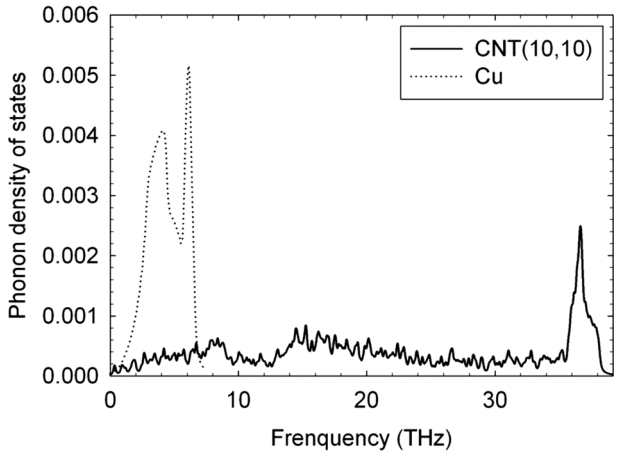

FIG. 4. The calculated phonon DOS of CNT(10,10) and Cu.

$$R_I = R_{Cu(e-p)} + R_{p-p} = \frac{1}{\kappa_{Cu(e-p)}} + \frac{1}{\kappa_{p-p}} = \left(\frac{1}{840} + \frac{1}{296}\right) \text{mm}^2\text{K/W} = 4.57 \times 10^{-3}\ \text{mm}^2\text{K/W}.$$

B. Thermal resistance along Path II

Along Path-II, the heat is transferred across the interface by direct electron-electron coupling at the metallic CNT/Cu interface, then is subsequently passed on to phonons via electron-phonons coupling within the CNT tube. Therefore, the thermal resistance along Path-II is the sum of the intrinsic thermal resistance associated with the electron-phonon coupling within the CNT tube ($R_{\text{CNT}(e\text{-}p)}$) and the resistance associated with direct electron-electron coupling at the interface (R_{e-e}), that is, $R_{II} = R_{CNT(e-p)} + R_{e-e}$.

For the direct electron-electron coupling at the CNT/Cu interface, quantum mechanics can be used to calculate the electron transmission coefficient across the interface. The Cu/CNT/Cu assembly was first optimized by using quantum mechanics to obtain its equilibrium static structure, see Fig. 5. Based on the Landauer formula, the electron-mediated thermal current or energy flux J_e across the CNT/Cu interface can be expressed as a function of electron transmission coefficient and temperature[16]

$$J_e = \frac{1}{\hbar}\int_{-\infty}^{+\infty} \frac{dE}{2\pi}(E-\mu)[f_F(E,T_L) - f_F(E,T_R)]\zeta_e(E), \quad (11)$$

where $f_F(E,T_{L/R})$ is the Fermi-Dirac distribution function for an electron with energy E in the left- or right-thermal reservoirs with the temperature $T_{L/R}$, respectively, μ is the averaged chemical potential between the hot and cold thermal reservoirs, and $\xi_e(E)$ is the transmission function for an incident electron with energy E. Therefore, the thermal conductance κ_{e-e} due to the direct electron-electron coupling at the interface can be derived as follows:

$$\kappa_{e-e}(T) = \frac{1}{\hbar}\frac{k_B}{\pi}\int_{-\infty}^{+\infty} dE\left(\frac{E-\mu}{k_BT}\right)^2 \frac{e^{(E-\mu)/k_BT}}{\left[e^{(E-\mu)/k_BT}+1\right]^2}\zeta_e(E), \quad (12)$$

where k_B is the Boltzmann constant and $T = (T_L + T_R)/2$ is the average temperature between the hot and cold thermal reservoirs. The transmission function can be computed through the independent $\mathbf{k}_{\text{II}}$ (surface-parallel direction reciprocal lattice vector point) channels and their integral over the 2D reciprocal unit cell, which can be calculated by the ATK-Toolkit software.[12]

$$T(E,V) = \frac{1}{\Omega}\int_{\tilde{\Omega}} d\mathbf{k}_{||} T^{\mathbf{k}_{||}}(E,V), \quad (13)$$

where Ω is the area of the reference unit cell surface. The matrix version of the non-equilibrium Green's function (NEGF) approach was used in the numerical simulation. The NEGF is a well-developed general formalism to treat various non-equilibrium charge transport phenomena.

The solid line shown in Fig. 6 is the calculated electron transmission coefficient spectrum of the Cu/CNT/Cu system as a function of energy level at 300 K. This result represents the end-contact system between metallic CNT(10,10) and Cu. The side-contact configuration will result in a significantly low electron transmission coefficient, as described in details in Ref. 37. Additionally, we also presented the calculated result of the Si/CNT(10,10)/Si system, which indicated that the electron-electron coupling at CNT/Si interface does not contribute to the thermal conductance because of the nearly zero transmission coefficient around Fermi level. Thus, in the Si/CNT(10,10)/Si interface system, it is reasonable to disregard the contribution from direct electron-electron coupling at the interface.

According to Eqs. (11) and (12), the thermal conductance due to direct electron-electron coupling at the CNT/Cu

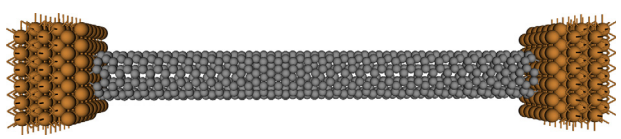

FIG. 5. (Color online) A typical Cu/CNT/Cu sandwich model for quantum mechanics calculations.

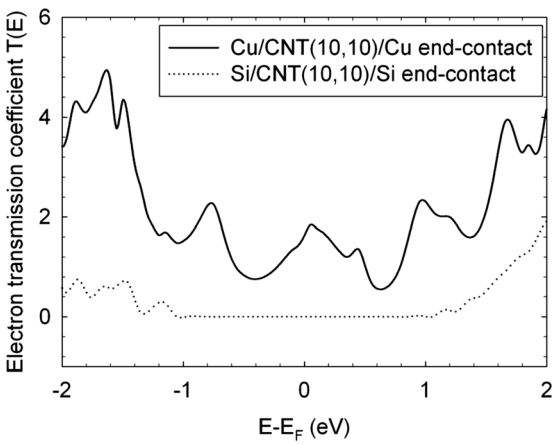

FIG. 6. The electron transmission coefficient $\xi_e(E)$ across the end-contact Cu/CNT(10,10)/Cu and Si/CNT(10,10)/Si interfaces. The Fermi level is located at 0 eV.

interface is $\kappa_{e-e} = 99.5\ \mathrm{W/mm^2\ K}$. This is relatively small compared with the phonon-phonon coupling at the interface.

The thermal conductance attributed to the electron-phonon coupling within the CNT tube can be derived in a manner similar to that within the Cu

$$\kappa_{CNT(e-p)} = \frac{1}{R_{CNT(e-p)}} = \sqrt{G \cdot \kappa_{p(CNT)}} = \sqrt{\left(C_{e(CNT)} \cdot \tau\right) \cdot \kappa_{p(CNT)}}. \quad (14)$$

The electron-phonon energy relaxation time τ is the time scale for an excited electron, with a typical excitation energy $\sim k_B T_e$, to relax back to the Fermi energy. It is inversely proportional to temperature, with the value of $\sim$1 ps for CNT at room temperature.[38,39] In addition, $C_{e(CNT)}$ is the electronic heat capacity of single-walled CNT(10,10), which can be calculated by the following equation:[17,40]

$$C_e = \frac{8\pi^2 L_0 k_B^2 T_e}{3hv_F}, \quad (15)$$

where L_0 is the length of the CNT tube, and T_e is the temperature. At room temperature, $G = (3/3.32) \times 10^{15}\ \mathrm{W/m^3K}$. The thermal conductivity of CNT(10,10) is taken as 3000 W/mK. Thus, according to Eq. (14), we have $\kappa_{CNT(e-p)} = 1.65 \times 10^9\ \mathrm{W/m^2\ K}$.

Finally, the total thermal resistance along Path-II can be calculated as

$$R_{II} = R_{CNT(e-p)} + R_{e-e} = \frac{1}{\kappa_{CNT(e-p)}} + \frac{1}{\kappa_{e-e}} = 1.06 \times 10^{-2}\ \mathrm{mm^2K/W}. \quad (16)$$

C. Total thermal resistance

The total thermal resistance of the junction between metallic CNT(10,10) and Cu can be computed from the resistance along both Path-I and Path-II. Based on the above analysis, the thermal resistance is $4.57 \times 10^{-3}\ \mathrm{mm^2\ K/W}$ along Path-I and $1.06 \times 10^{-2}\ \mathrm{mm^2\ K/W}$ along Path-II. Since Path-I and Path-II are in parallel, see Fig. 1, the total thermal resistance R_{total} is thus

$$R_{total} = \frac{R_I R_{II}}{R_I + R_{II}} = 3.19 \times 10^{-3}\ \mathrm{mm^2K/W}. \quad (17)$$

This value is very close to the reported value ($3.0 \times 10^{-3}\ \mathrm{mm^2\ K/W}$) for the contact between an individual CNT and a Cu substrate based on a continuum model.[41] The ballistic resistance for metal-metal interfaces measured at room temperature is $\sim 10^{-3}\ \mathrm{mm^2\ K/W}$,[42] which is also in good agreement with the value obtained in our study.

IV. SUMMARY AND CONCLUSIONS

In conclusion, a new model is proposed in this study to calculate the thermal resistance between metallic CNT and metal substrate, which accounts for the direct electron-electron coupling and phonon-phonon coupling at the interface, as well as the electron-phonon coupling within CNT and Cu. The following conclusions can be drawn.

(1) The total thermal transfer across a metallic CNT(10,10)/Cu system consists of two contributions in parallel. One (Path-I) is caused by the electron-phonon coupling within Cu, and the subsequent phonon-phonon coupling at the CNT/Cu interface. The other (Path-II) is the direct electron-electron coupling at the CNT/Cu interface and the subsequent electron-phonon coupling within the CNT tube.

(2) Our results show that the thermal resistance along Path-I is $4.57 \times 10^{-3}\ \mathrm{mm^2\ K/W}$, and that along Path-II is $1.06 \times 10^{-2}\ \mathrm{mm^2\ K/W}$. These give $R_{total} = 3.19 \times 10^{-3}\ \mathrm{mm^2\ K/W}$, which is consistent with the existing results in the literature.

(3) The model developed here provides a systematic approach to study the thermal resistance between metallic CNT and metal substrate based on the atomic-level simulations.

It is noteworthy that the different computational methods used in this study have their own limitations and regimes of applicability. The MD method for simulating phonon transport is a classical method that neglects the quantum effects. The NEGF method herein for calculating electron transmission coefficient, on the other hand, assumes coherent transport without accounting for the interaction between electron and phonon (or photon).

ACKNOWLEDGMENTS

The work is supported in part by DARPA through Contract No. N66001-09-C-2012. The view expressed are those of the author and do not reflect the official policy or position of the Department of Defense or the US Government.

[1] X. J. Hu, A. A. Padilla, J. Xu, T. S. Fisher, and K. E. Goodsen, J. Heat Transfer-Trans. ASME **128**(11), 1109 (2006).
[2] S. U. S. Choi, Z. G. Zhang, W. Yu, F. E. Lockwood, and E. A. Grulke, Appl. Phys. Lett. **79**(14), 2252 (2001).
[3] Q. Ngo, B. A. Cruden, A. M. Cassell, G. Sims, M. Meyyappan, J. Li, and C. Y. Yang, Nano Lett. **4**(12), 2403 (2004).
[4] L. B. Zhu, Y. Y. Sun, D. W. Hess, and C.-P. Wong, Nano Lett. **6**(2), 243 (2006).
[5] S. Banerjee, T. Hemraj-Benny, and S. S. Wong, Advanced Materials **17**(1), 17 (2005).
[6] B. S. Flavel, J. X. Yu, J. G. Shapter, and J. S. Quinton, Carbon **45**(13), 2551 (2007).
[7] J. X. Yu, J. G. Shapter, J. S. Quinton, M. R. Johnston, and D. A. Beattie, Phys. Chem. Chem. Phys. **9**(4), 510 (2007).
[8] J. Diao, D. Srivastava, and M. Menon, J. Chem. Phys. **128**(16), 2905211 (2008).
[9] H. B. Fan, K. Zhang, and M. M. F. Yuen, J. Appl. Phys. **106**(3), 034307 (2009).
[10] Z. Y. Ong and E. Pop, Phys. Rev. B **81**(15), 155408 (2010).
[11] M. Hu, P. Keblinski, J.-S. Wang, and N. Raravikar, J. Appl. Phys. **104**(8), 083503 (2008).
[12] F. Gao, J. M. Qu, and M. Yao, Appl. Phys. Lett. **97**(24), 242112 (2010).
[13] A. Majumdar and P. Reddy, Appl. Phys. Lett. **84**(23), 4768 (2004).
[14] Q. W. Li, C. H. Liu, and S. S. Fan, Nano Letters **9**(11), 3805 (2009).
[15] B. C. Gundrum, D. G. Cahill, and R. S. Averback, Phys. Rev. B **72**(24), 245426 (2005).
[16] T. Yamamoto, Y. Nakazawa, and K. Watanabe, New J. Phys. **9**, 245 (2007).
[17] D. F. Santavicca, J. D. Chudow, D. E. Prober, M. S. Purewal, and P. Kim, Nano Lett. **10**(11), 4538 (2010).
[18] R. J. Stoner and H. J. Maris, Phys. Rev. B **47**(18), 11826 (1993).
[19] H. K. Lyeo and D. G. Cahill, Phys. Rev. B **73**(14), 144301 (2006).

[20]N. Stojanovic, D. H. S. Maithripala, J. M. Berg, and M. Holtz, Phys. Rev. B **82**(7), 075418 (2010).
[21]H. E. Elsayed-Ali, T. B. Norris, M. A. Pessot, and G. A. Mourou, Phys. Rev. Lett. **58**(12), 1212 (1987).
[22]J. Shiomi and S. Maruyama, Int. J. Thermophys. **31**(10), 1945 (2010).
[23]J. A. Thomas, J. E. Turney, R. M. Lutzi, C .H. Amon, and A. J. H. McGaughey, Phys. Rev. B **81**(8), 081411 (2010).
[24]J. S. Wang, Phys. Rev. Lett. **99**(16), 160601 (2007).
[25]J. A. Thomas, R. M. Iutzi, and A. J. H. McGaughey, Phys. Rev. B **81**(4), 045413 (2010).
[26]H. L. Zhong and J. R. Lukes, Phys. Rev. B **74**(12), 125403 (2006).
[27]P. Jund and R. Jullien, Phys. Rev. B **59**(21), 13707 (1999).
[28]J. Tersoff, Phys. Rev. Lett. **61**(25), 2879 (1988).
[29]J. Tersoff, Phys. Rev. B **37**(12), 6991 (1988).
[30]D. W. Brenner, Phys. Rev. B **42**(15), 9458 (1990).
[31]L. Lindsay and D.A. Broido, Phys. Rev. B **81**(20), 205441 (2010).
[32]B. J. Lee, J. H. Shim, and M. I. Baskes, Phys. Rev. B **68**(14), 144112 (2003).
[33]Q. X. Pei, C. Lu, F. Z. Fang, and H. Wu, Comput. Mater. Sci. **37**(4), 434 (2006).
[34]J. R. Lukes and H. L. Zhong, J. Heat Trans.-Trans. ASME **129**(6), 705 (2007).
[35]R. J. Stevens, L. V. Zhigilei, and P. M. Norris, Int. J. Heat Mass Transfer **50**(19-20), 3977 (2007).
[36]E. T. Swartz and R. O. Pohl, Rev. Mod. Phys. **61**(3), 605 (1989).
[37]F. Gao, J. M. Qu, and M. Yao, Appl. Phys. Lett. **98**(17), 172103 (2011).
[38]R. A. Jishi, M. S. Dresselhaus, and G. Dresselhaus, Phys. Rev. B **48**(15), 11385 (1993).
[39]J. Y. Park, S. Rosenblatt, Y. Yaish, V. Sazonova, H. Ustunel, S. Braig, T. A. Arias, P. W. Brouwer, and P. L. McEuen, Nano Lett. **4**(3), 517 (2004).
[40]L. X. Benedict, S. G. Louie, and M. L. Cohen, Solid State Communications **100**(3), 177 (1996).
[41]B. A. Cola, J. Xu, and T. S. Fisher, Int. J. Heat Mass Transfer **52**(15–16), 3490 (2009).
[42]B. M. Clemens, G. L. Eesley, and C. A. Paddock, Phys. Rev. B **37**(3), 1085 (1988).